Enhanced Sommerfeld coefficient near the quantum critical point in YbMn6Ge6-xSnx

P. Haraux, Lucas Eichenberger, L. V. B. Diop, T. Mazet

▶ **To cite this version:**

P. Haraux, Lucas Eichenberger, L. V. B. Diop, T. Mazet. Enhanced Sommerfeld coefficient near the quantum critical point in YbMn6Ge6-xSnx. Solid State Communications, 2022, 341, pp.114551. ⟨10.1016/j.ssc.2021.114551⟩. ⟨hal-03821282⟩

HAL Id: hal-03821282

https://hal.science/hal-03821282v1

Submitted on 19 Oct 2022

HAL is a multi-disciplinary open access archive for the deposit and dissemination of scientific research documents, whether they are published or not. The documents may come from teaching and research institutions in France or abroad, or from public or private research centers.

L'archive ouverte pluridisciplinaire **HAL**, est destinée au dépôt et à la diffusion de documents scientifiques de niveau recherche, publiés ou non, émanant des établissements d'enseignement et de recherche français ou étrangers, des laboratoires publics ou privés.

HAL Authorization

Enhanced Sommerfeld coefficient near the quantum critical point in $YbMn_6Ge_{6-x}Sn_x$

P. Haraux[a], L. Eichenberger[a], L.V.B. Diop[a], T. Mazet[a,*]

[a] *Université de Lorraine, CNRS, IJL, F-54000 Nancy, France*

Abstract

We investigate the $YbMn_6Ge_{6-x}Sn_x$ alloys ($4.00 \leq x \leq 5.55$) by means of specific heat measurements in the temperature range 1.9 to 200 K. For x near ~ 4.0, the Sommerfeld coefficient γ is close to that of a Lu-based counterpart ($\gamma \sim 40$ mJ.mole^{-1}.K^{-2}). The γ coefficient increases upon Sn for Ge substitution, enters the heavy fermion regime and peaks ($\gamma \sim 210$ mJ.mole^{-1}.K^{-2}) in the vicinity of the Yb magnetic instability ($x_c \sim 5.23$), before diminishing upon further Sn content increase. The enhanced γ values near x_c agree with the close proximity of a quantum critical point previously inferred from electronic spectroscopy experiments.

Keywords: A. Yb-based intermetallics D. heavy fermion quantum criticality E. Specific heat

1. Introduction

Strongly correlated electrons materials are intensively studied since they offer the possibility of stabilizing new and exotic ground states [1]. Among the numerous correlated materials families (high-T_c cuprates and other oxides, heavy fermion systems, low-dimension materials ...), $4f$ electron heavy fermion systems have the advantage to involve small energy scales that can be easily tuned by control parameters such as external pressure, magnetic field or chemical composition [2].

In the vast majority of $4f$ heavy fermion compounds and alloys studied so far, the anomalous rare-earth (mainly Ce or Yb) is alloyed with non-magnetic

*Corresponding author

elements [2, 3]. The ground state then results from the competition between two interactions that depend differently on the hybridization between the localized $4f$ states and the conduction electrons [4]: the Kondo effect, which tends to demagnetize the system, and the Ruderman-Kittel-Kasuya-Yosida (RKKY) interaction that promotes magnetic order. Depending on the strength of the hybridization, various ground states can be realized (magnetically ordered, heavy fermion, intermediate valent...). When the RKKY and Kondo interactions are of comparable magnitude, the magnetic ordering is suppressed to absolute zero temperature, which corresponds to a quantum critical point (QCP) [5]. The quantum fluctuations at the QCP yields profound modifications in metal properties, even at finite temperature, such as non-Fermi-liquid behavior or unconventional superconductivity.

When Yb is alloyed with non-magnetic elements, the QCP occurs in most cases for nearly trivalent Yb (one of the most prominent counter-examples being β-$YbAlB_4$ [6, 7]) and the quantum critical effects are perceived only at low temperatures [1, 2, 3].

A few years ago, we identified and started to investigate a system where intermediate valent Yb and a magnetized $3d$ sublattice coexist, namely $YbMn_6Ge_{6-x}Sn_x$, using magnetization, neutron diffraction and spectroscopy experiments [8, 9, 10, 11, 12]. These hexagonal phases ($P6/mmm$, $HfFe_6Ge_6$-type) comprise a single site for the Mn atoms ($6i$) and Yb atoms ($1b$) and three sites for the p element ($2c$, $2d$ and $2e$). In this system, the Yb valence decreases (i.e. the $4f$ conduction electron hybridization is enhanced) through chemical pressure reduction upon Sn for Ge substitution [9, 10, 12]. Yb is (almost) trivalent in $YbMn_6Ge_6$ [10], while its valency is $\nu \sim 2.59$ in $YbMn_6Sn_6$ [12]. The low-temperature Yb magnetic order disappears for $x > 5.23$ when Yb is in the intermediate valence regime ($\nu \sim 2.77$) [12]. The Mn sublattice magnetically orders at or above room-temperature and its behavior depends on the R = Yb valence [8, 11], a well-documented behavior in the wide RMn_6X_6 family (X = Ge, Sn) [13, 14, 15]. In the Ge-rich $YbMn_6Ge_{6-x}Sn_x$ alloys, the Mn sublattice is basically antiferromagnetic. Upon reducing the Yb valence through Sn for Ge substitution, a ferromagnetic region develops in the (x, T) phase diagram and the Mn sublattice is ferromagnetic over the whole ordered temperature range for $x > 4.65$ (see Fig. 4 of Ref. [11]).

Besides the Yb magnetic instability occurring at strong hybridization mentioned above, the $YbMn_6Ge_{6-x}Sn_x$ alloys exhibit several other singular Yb behaviors which have been ascribed to the magnitude of the Mn-Yb exchange interaction [9, 11, 12], quite stronger than the usual Yb-Yb RKKY

interaction [16]. The Yb valence tends to increase upon cooling [9] at odds to the usual behavior [17]. The Yb magnetic ordering of Yb reaches the record value $T_{Yb} \sim 125$ K for $x = 4.65$ while, to the best of our knowledge, the highest Yb magnetic transition temperature otherwise observed is 32 K in β-$YbAlB_4$ under the external pressure of 8 GPa [7]. Finally, the peak in the composition dependence of the Yb valence (at 300 and 5 K) and XMCD signal (at 5 K) near $x_c \sim 5.23$ has been analyzed as possible signatures of $4f$ quantum criticality [12]. Thus, β-$YbAlB_4$ [7] and $YbMn_6Ge_{6-x}Sn_x$ share the common feature of having a QCP in the intermediate valence regime ($\nu \sim 2.75$ [6] *vs.* $\nu \sim 2.77$ [12], respectively).

None of these works on $YbMn_6Ge_{6-x}Sn_x$ are based on thermodynamic or transport measurements, valuable -if not indispensable- tools for studying heavy fermion behaviors and $4f$ electron quantum criticality. To partially fill this gap, we investigate here the $YbMn_6Ge_{6-x}Sn_x$ alloys (with $4.00 \leq x \leq 5.55$) using specific heat measurements with the motivation of a better understanding of the $4f$ electrons behavior in this series.

2. Experimental details

Most of the $YbMn_6Ge_{6-x}Sn_x$ used in this study are from the same batches as those employed previously Refs. [11, 12]. A few supplementary Yb-based polycristalline alloys were prepared as described in reference [8]. Two representative X-ray diffraction patterns (D8 Advance, Bruker, $\lambda = 1.54056$ Å) are shown in figure 1. A single crystal with composition $YbMn_6Ge_{1.91}Sn_{4.09}$, as determined by X-ray diffraction, was grown in Sn flux [18, 19]. The elements were placed in a quartz tube, in the ratio Yb:Mn:Ge:Sn=1:6:0.8:30, which was sealed under pure Ar atmosphere (0.25 atm.). The materials were heated to 1000 °C and kept there for four hours. The temperature was then reduced to 600 °C at a rate of 6 °C h^{-1}. The excess Sn flux was removed by centrifugation. This yielded single crystals in the form of hexagonal prisms with typical volume of ~ 1 mm^3. Note that, using this protocol, we did not yet succeed in growing single crystals with composition close to that of the Yb magnetic instability ($x_c \sim 5.23$) and only crystals with x close to 4 have been obtained even with widely varying the Ge content of the flux.

Specific heat measurements $C_p(T)$ were performed by a relaxation method using a Physical Properties Measurements System (PPMS, Quantum Design) [20, 21]. Most of the samples were investigated from 200 K down to 1.9 K while some of them were investigated only below 20 K. For the single crystal

($x = 4.09$), the data presented here were obtained with one hexagonal face in contact with the sample platform. Data obtained in the perpendicular orientation are identical.

A Lu-based polycristalline sample with composition $LuMn_6Ga_{0.8}Sn_{5.2}$ was prepared in similar conditions to the Yb-based ones in order to allow for comparison of their Sommerfeld coefficients γ. In this compound, the Mn sublattice is ferromagnetic over the whole ordered temperature range ($T_C \sim$ 340 K) [22, 23], as in $YbMn_6Ge_{6-x}Sn_x$ with $x > 4.65$, while $LuMn_6(Ge,Sn)_6$ alloys are antiferromagnets with a possible commensurate - incommensurate transition [24] that might yield parasitic anomalies in the $C_p(T)$ data.

3. Results and discussion

The temperature variation of the specific heat of some $YbMn_6Ge_{6-x}Sn_x$ alloys is shown in figure 2. Two specific heat anomalies are observed for $x \leq$ 4.45. The one near $\sim$ 120 K that weakly shifts towards lower temperature upon increasing x. The second one, at lower temperature, that goes to higher temperature and reduces in intensity upon increasing x. The high temperature peak is associated with changes in the Mn spins arrangement, from helimagnetic to skewed spiral upon cooling, previously detected by neutron diffraction [8, 11]. It is no longer observed in richer Sn alloys since the Mn sublattice is then ferromagnetic over the whole ordered temperature range. The low-temperature specific heat anomaly corresponds to the the magnetic ordering of Yb. The Yb magnetic ordering temperature is known to increase with x up to $T_{Yb} \sim 125$ K for $x = 4.65$, before decreasing down to its suppression for $x \sim 5.23$ [11, 12]. However, no corresponding specific heat anomaly is seen for $x > 4.65$, likely because the magnetic entropy associated with the then strongly reduced Yb magnetic moment ($< 0.30\ \mu_B$ [11]) is too low.

The electronic specific heat (Sommerfeld) coefficient, γ, and the Debye temperature, Θ_D, were obtained by least-squares fitting of the low temperature C_p/T vs. T^2 data (figure 3). The C_p/T curve of all polycristalline samples comprises a peak near 2 K that is absent in the heat capacity data of the single crystal ($x = 4.09$), as shown in the inset of figure 3. This peak is unambiguously due small amounts of Yb_2O_3 which orders antiferromagnetically at $T_N \sim 2.3$ K [25]. The Yb_2O_3 impurity is often present in Yb-based intermetallic polycristalline samples [26, 27, 28] and, from our own experience, can hardly be avoided in the $YbMn_6Ge_{6-x}Sn_x$ series. Attempts to subtract the Yb_2O_3 contribution to the total specific heat using C_p data

of commercial oxide were not satisfactory, the peak shape and exact temperature maximum being different to those of commercial Yb_2O_3 and somewhat sample dependent. We therefore restricted the linear regression of the data, in the form $C_p/T = \gamma + \beta T^2$, to temperatures higher than 7 K where the magnetic contribution of the oxide is negligible.

The fitted slope β allows calculating the Debye temperature using the relationship [29]:

$$\Theta_D^3 = \frac{12\pi^4 nR}{5\beta}$$

where R is the gas constant and n the number of atoms in a formula unit (here $n = 13$). The fits results in Θ_D values decreasing slightly and steadily with increasing Sn content from $\Theta_D \sim 260$ K for $x = 4$ down to $\Theta_D \sim 240$ K for $x = 5.55$ (see inset of figure 4). That can be explained by a weakening of the chemical bonds in the Mn-[Yb,Sn/Ge($2d$)]-Mn slab upon Sn for Ge substitution. In the investigated composition range ($4 < x < 6$), the $2c$ and $2e$ metalloid sites are full of Sn atoms and the Sn for Ge substitution occurs only on the $2d$ site [8, 11]. The replacement of Ge by larger Sn results in a weakening of the Mn-metalloid chemical bonds and, in addition, the concomitant reduction of $5d$ electrons count on Yb - associated with the lowering of the Yb valence - weakens the Mn-Yb bonds. A similar decrease of the Debye temperature and Yb valence upon substitution with a larger isoelectronic element has been observed for instance in $YbFe_2Zn_{20-x}Cd_x$ [30].

The composition dependence of γ is less regular (figure 4). For compositions near $x \sim 4.0$, $\gamma \sim 40$ mJ.mole^{-1}.K^{-2}, close to that of $LuMn_6Ga_{0.8}Sn_{5.2}$. This indicates that at this Sn content, when Yb is almost trivalent [12], there is no renormalization of the effective mass m^* of the charge carriers. Upon x increase, γ value becomes larger, goes to a maximum ($\gamma \sim 210$ mJ.mole^{-1}.K^{-2}) for x close to the Yb magnetic instability ($x_c \sim 5.23$ [11]), before decreasing a little ($\gamma \sim 150$ mJ.mole^{-1}.K^{-2} for $x = 5.55$). Concomitantly, the previously found Yb valence ν reduces upon x increase but peaks close to the Yb magnetic instability ($x_c \sim 5.23$), which has been analyzed as a signature of quantum criticality [12].

The $YbMn_6Ge_{6-x}Sn_x$ alloys with $x \gtrsim 5$ are moderately heavy fermion materials with $\gamma > 100$ mJ.mole^{-1}.K^{-2}. Since $\gamma \propto m^* \propto 1/T_K$, genuine heavy fermion behaviors are generally observed for almost trivalent Yb [3, 31, 32] and, in a series of compounds, the Sommerfeld coefficient tends to reduce with the Yb valence [26, 27, 28, 33]. In $YbMn_6Ge_{6-x}Sn_x$, the increase of γ

whilst the Yb valence reduces (i.e. the Kondo temperature T_K increases) is somewhat unusual and at odds to expected dependence of T_K vis-a-vis the hybridization between the $4f$ states and conduction electrons.

Enhanced effective mass m^* is one of the usual signatures of quantum criticality [1, 2] and has been experimentally observed for instance in $CeNi_{1-x}Ni_xGe_2$ [34]. Hence, the enhanced Sommerfeld coefficients near $x_c \sim 5.23$ agree with the conclusion of the spectroscopic study about the vicinity a QCP, deep in the intermediate valence regime [12]. The low-temperature limit of our measurements (1.9 K) and the presence of the Yb_2O_3 impurity, which overshadows the main phase behavior below $\sim$ 7 K, do not allow determining $\gamma(T \rightarrow 0)$ nor evidencing a possible non-Fermi-liquid behavior (e.g. a divergence of the magnetic specific heat on approaching 0 K), another hallmark of quantum criticality [2, 3].

4. Conclusion

Our results show that charge carriers in $YbMn_6Ge_{6-x}Sn_x$ with $x \gtrsim 5$ are heavy fermion particles. Further, the enhanced effective mass m^* near x_c confirms that the Yb magnetic instability corresponds to a quantum critical point, as previously inferred from spectroscopic experiments. A better understanding of the physics near the quantum critical point now requires C_p measurements below 1.9 K as well as transport measurements (resistivity, thermoelectric power) carried out, preferably, on single crystals.

References

[1] S. Paschen and Q. Si, Nat. Rev. Phys. 3 (2021) 9.

[2] S. Wirth and F. Steglich, Nat. Rev. Mater. 1 (2016) 1.

[3] P. Coleman, H. Kronmüller and S. Parkin (Eds.), *Heavy Fermions: Electrons at the Edge of Magnetism*, Handbook of Magnetism and Advanced Magnetic Materials, Wiley, New York, 2007.

[4] S. Doniach, Physica B 91 (1977) 231.

[5] S. Sachdev, Nat. Phys. 4 (2008) 173.

[6] M. Okawa, M. Matsunami, K. Ishizaka, R. Eguchi, M. Taguchi, A. Chainani, Y. Takata, M. Yabashi, K. Tamasaku, Y. Nishiro, T. Ishikawa, K. Kuga, N. Horie, S. Najkatsuji, and S. Shin, Phys. Rev. Lett. 104 (2010) 247201.

[7] T. Tomita, K. Kuga, Y. Uwatoko, and S. Nakatsuji, Phys. Rev. B 94 (2016) 245130.

[8] T. Mazet, H. Ihou-Mouko, D.H. Ryan, C.J. Voyer, J.M. Cadogan and B. Malaman, J. Phys.: Condens. Matter 22 (2010) 116005.

[9] T. Mazet, D. Malterre, M. François, C. Dallera, M. Grioni and G. Monaco, Phys. Rev. Lett. 111 (2013) 096402.

[10] T. Mazet, D. Malterre, M. François, L. Eichenberger, C. Dallera, M. Grioni and G. Monaco, Phys. Rev. B 92 (2015) 075105.

[11] L. Eichenberger, D. Malterre, B. Malaman and T. Mazet, Phys. Rev. B 96 (2017) 155129.

[12] L. Eichenberger, A. Magnette, D. Malterre, R. Sibille, F. Baudelet, L. Nataf and T. Mazet, Phys. Rev. 101 (2020) 020408(R).

[13] T. Mazet, G. Venturini, R. Welter, B. Malaman, J. Alloys Compd. 264 (1998) 71.

[14] T. Mazet, O. Isnard and B. Malaman, J. Phys.: Condens. Matter 17 (2005) 1547.

[15] T. Mazet, H. Ihou-Mouko, J.F. Marêché, B. Malaman, Solid State Commun. 147 (2007) 659.

[16] M.S.S. Brooks, L. Nordström, and B. Johansson, J. Phys.: Condens. Matter 3 (1991) 2357.

[17] N.E. Bickers, D.L. Cox, and J.W. Wilkins, Phys. Rev. B 36 (1987) 2036.

[18] P.C. Canfield and Z. Fisk, Philos. Mag. B 65 (1992) 1117.

[19] D.M. Clatterbuck, K.A. Gschneidner Jr., J. Magn. Magn. Mater. 207 (1999) 78.

[20] J.S. Hwang, K.L. Lin, and C. Tien, Rev. Sci. Instrum. 68 (1997) 94.

[21] J.C. Lashley, M.F. Hundley, A. Migliori, J.L. Sarrao, P. G. Pagliuso, T.W. Darling, M. Jaime, J.C. Cooley, W.L. Hults, L. Morales, D.J. Thoma, J.L. Smith, J. Boerio-Goates, B.F. Woodfield, G.R. Stewart, R.A. Fisher, N.E. Phillips, Cryogenics 43 (2003) 369.

[22] C. Lefèvre, 2004, *Thèse de l'Université Nancy I*, Nancy, France.

[23] F. Canepa, R. Duraj, C. Lefèvre, B. Malaman, A. Mar, T. Mazet, M. Napoletano, A. Szytula, J. Tobola, G. Venturini, A. Vernière, J. Alloys Compd. 383 (2004) 10.

[24] G. Venturini, D. Fruchart, B. Malaman, J. Alloys Compd. 236 (1996) 102.

[25] R.M. Moon, W.C. Koelher, H.R. Child, and L.J. Raubenheimer, Phys. Rev. 176 (1968) 722.

[26] E. Bauer, Le Tuan, R. Hauser, E. Gratz, T. Holubar, G. Hilscher, H. Michor, W. Perthold, C. Godart, E. Alleno, K. Hiebl, Phys. Rev. B 52 (1995) 4327.

[27] E. Bauer, R. Hauser, L. Keller, P. Fischer, O. Trovarelli, J.G. Sereni, J.J. Rieger and G.R. Stewart, Phys. Rev. B 56 (1997) 711.

[28] B.K. RaI, I.W.H. Oswald, J.Y. Chan, and E. Morosan, Phys. Rev. B 93 (2016) 035101.

[29] G.R. Stewart, Rev. Mod. Phys. 56 (1984) 755.

[30] M. Cabrera-Baez, R.A. Ribeiro and M.A. Avila, J. Phys.: Condens. Matter 28 (2016) 375601.

[31] N. Tsujii, H. Kitazawa, Solid State Commun. 159 (2013) 65.

[32] C. Rossel, K.N. Yang, M.B. Maple, Z. Fisk, E. Zirngiebl, and J.D. Thompson, Phys. Rev. B 35 (1987) 1914.

[33] W.B. Jiang, L. Yang, C.Y. Guo, Z. Hu, J.M. Lee, M. Smidman, Y.F. Wang, T. Shang, Z.W. Cheng, F. Gao, H. Ishii, K.D. Tsueri, Y.F. Liao, X. Lu, L.H. Tjeng, J.M. chen and H.Q. Yuan, Sci. Rep. 5 (2015) 17608.

[34] B.K. Lee, J.B. Hong, J.W. Kim, Kwang-hyun Jang, E.D. Mun, M.H. Jung, S. Kimura, Tuson Park, J.-G. Park, Y.S. Kwon, Phys. Rev. B 71 (2005) 214443.

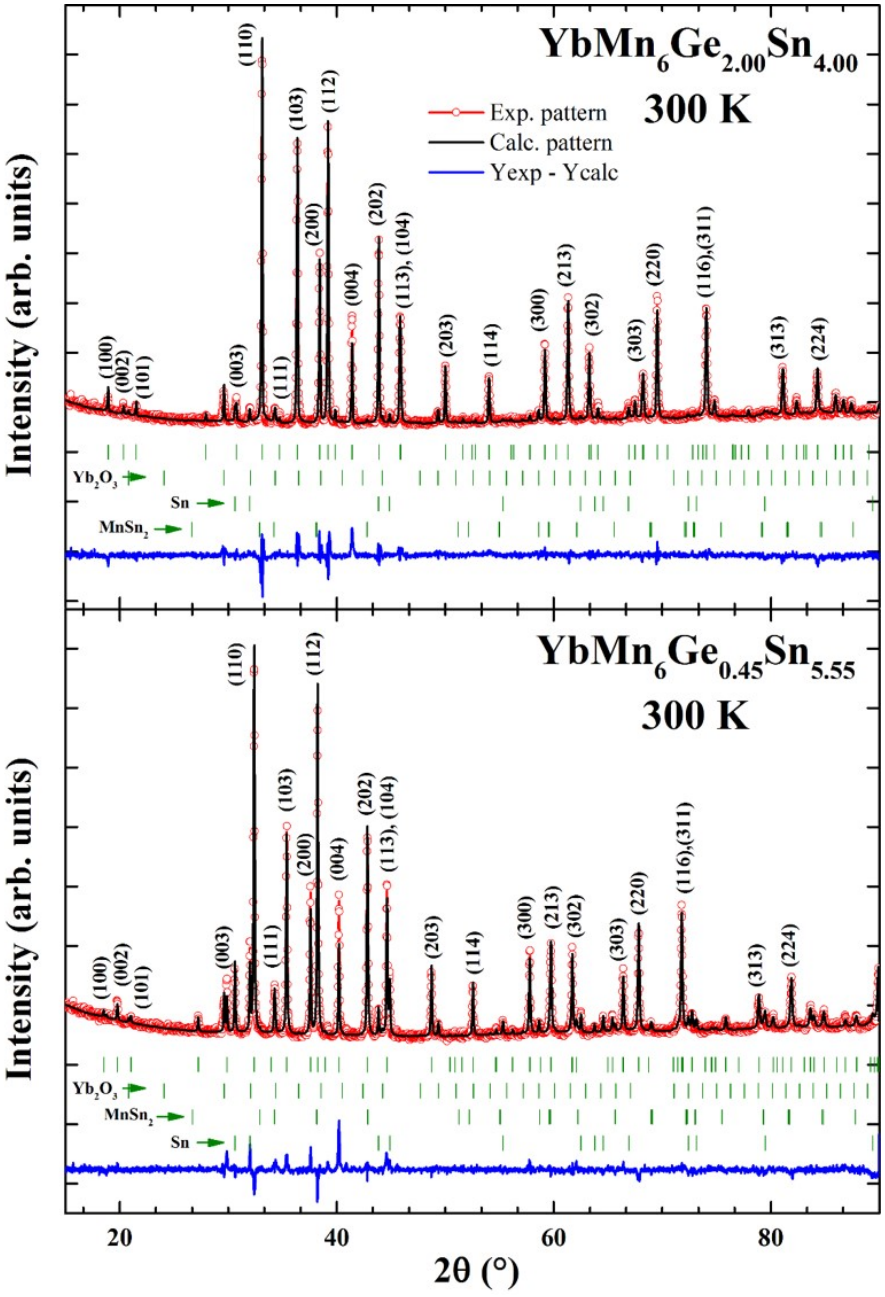

Figure 1: Refined X-ray diffraction pattern of $YbMn_6Ge_{6-x}Sn_x$ for a) $x = 4.00$ and b) $x = 5.55$.

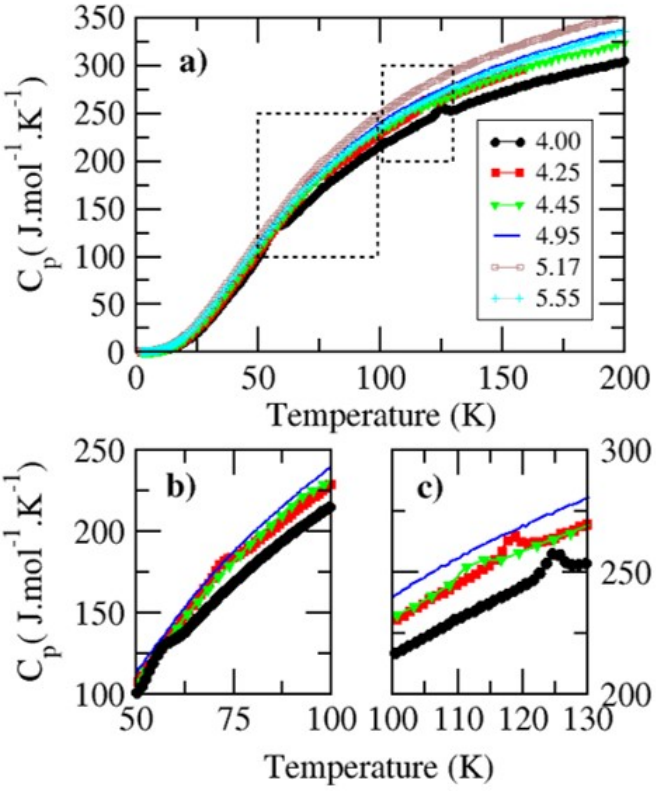

Figure 2: a) Temperature variation of the specific heat of $YbMn_6Ge_{6-x}Sn_x$ between 1.9 and 200 K. b) and c) Zoom on the 50-100 K and 100-130 K temperature range, respectively, for the alloys with $4.00 \leq x \leq 4.95$.

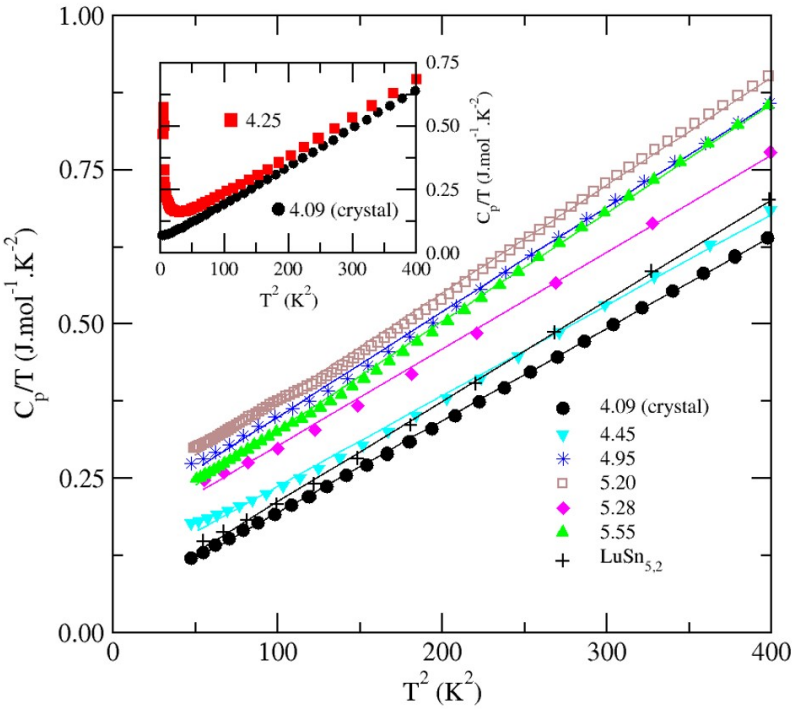

Figure 3: The C_p/T vs. T^2 plot for $YbMn_6Ge_{6-x}Sn_x$ and $LuMn_6Ga_{0.8}Sn_{5.2}$ from $\sim$ 7 K (50 K^2) to $\sim$ 20 K (400 K^2). The straight lines correspond to the least-squares fits. The inset shows C_p/T vs. T^2 data down to $\sim$ 1.9 K for $x = 4.09$ (single crystal) and $x = 4.25$ (polycrystal).

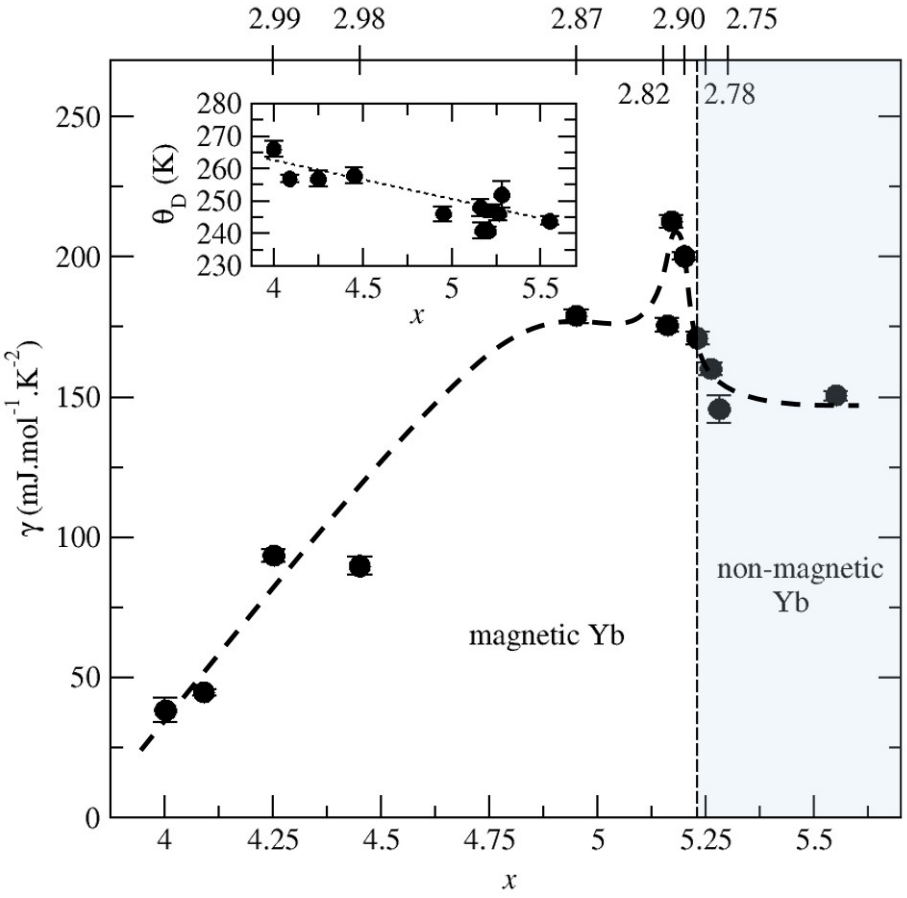

Figure 4: Composition dependence of the Sommerfeld coefficient γ in $YbMn_6Ge_{6-x}Sn_x$. Some Yb valence values at 5 K taken from reference [12] are indicated on the top axis. The thin vertical line marks the Yb magnetic instability [11, 12]. The dashed curved line is a guide to the eye. The inset shows the composition dependence of the Debye temperature Θ_D. The dotted straight line is a guide to the eye